

# Coherence properties of spontaneous parametric down-conversion pumped by a multi-mode cw diode laser

Osung Kwon, Young-Sik Ra, and Yoon-Ho Kim

Department of Physics, Pohang University of Science and Technology (POSTECH), Pohang,  
790-784, Korea

[yooho@postech.ac.kr](mailto:yooho@postech.ac.kr)

<http://qopt.postech.ac.kr>

**Abstract:** Coherence properties of the photon pair generated via spontaneous parametric down-conversion pumped by a multi-mode cw diode laser are studied with a Mach-Zehnder interferometer. Each photon of the pair enters a different input port of the interferometer and the biphoton coherence properties are studied with a two-photon detector placed at one output port. When the photon pair simultaneously enters the interferometer, periodic recurrence of the biphoton de Broglie wave packet is observed, closely resembling the coherence properties of the pump diode laser. With non-zero delays between the photons at the input ports, biphoton interference exhibits the same periodic recurrence but the wave packet shapes are shown to be dependent on both the input delay as well as the interferometer delay. These properties could be useful for building engineered entangled photon sources based on diode laser-pumped spontaneous parametric down-conversion.

© 2009 Optical Society of America

**OCIS codes:** (270.1670) Coherent optical effects; (270.5565) Quantum communications; (270.5290) Photon statistics; (270.5585) Quantum information and processing

---

## References and links

1. J. P. Dowling and G. J. Milburn, "Quantum technology: the second quantum revolution," *Phil. Trans. R. Soc. Lond. A* **361**, 1655-1674 (2003).
2. N. Gisin, G. Ribordy, W. Tittel, and H. Zbinden, "Quantum cryptography," *Rev. Mod. Phys.* **74**, 145-195 (2002).
3. P. Kok, W. J. Munro, K. Nemoto, T. C. Ralph, J. P. Dowling, and G. J. Milburn, "Linear optical quantum computing with photonic qubits," *Rev. Mod. Phys.* **79**, 135-174 (2007).
4. Y. H. Shih and C. O. Alley, "New Type of Einstein-Podolsky-Rosen-Bohm Experiment Using Pairs of Light Quanta Produced by Optical Parametric Down Conversion," *Phys. Rev. Lett.* **61**, 2921-2924 (1988).
5. P. G. Kwiat, K. Mattle, H. Weinfurter, A. Zeilinger, A. V. Sergienko, and Y. H. Shih, "New High-Intensity Source of Polarization-Entangled Photon Pairs," *Phys. Rev. Lett.* **75**, 4337-4341 (1995).
6. Y.-H. Kim, S. P. Kulik, M. V. Chekhova, W. P. Grice, and Y. Shih, "Experimental entanglement concentration and universal Bell-state synthesizer," *Phys. Rev. A* **67**, 010301(R) (2003).
7. J. G. Rarity and P. R. Tapster, "Experimental Violation of Bell's Inequality Based on Phase and Momentum," *Phys. Rev. Lett.* **64**, 2495-2498 (1990).
8. D. V. Strekalov, T. B. Pittman, A. V. Sergienko, Y. H. Shih, and P. G. Kwiat, "Postselection-free energy-time entanglement," *Phys. Rev. A* **54**, R1-R4 (1996).
9. W. P. Grice, A. B. U'Ren, and I. A. Walmsley, "Eliminating frequency and space-time correlations in multiphoton states," *Phys. Rev. A* **64**, 063815 (2001).
10. Y.-H. Kim and W. P. Grice, "Generation of pulsed polarization-entangled two-photon state via temporal and spectral engineering," *J. Mod. Opt.* **49**, 2309-2323 (2002).

11. A. Valencia, A. Cere, X. Shi, G. Molina-Terriza, and J. P. Torres, "Shaping the Waveform of Entangled Photons," *Phys. Rev. Lett.* **99**, 243601 (2007).
12. P. J. Mosley, J. S. Lundeen, B. J. Smith, P. Wasylczyk, A. B. U'Ren, C. Silberhorn, and I. A. Walmsley, "Heralded Generation of Ultrafast Single Photons in Pure Quantum States," *Phys. Rev. Lett.* **100**, 133601 (2008).
13. P. G. Kwiat, E. Waks, A. G. White, I. Appelbaum, and P. H. Eberhard, "Ultrabright source of polarization-entangled photons," *Phys. Rev. A* **60**, R773-R776 (1999).
14. Y.-H. Kim, M. V. Chekhova, S. P. Kulik, M. H. Rubin, and Y. Shih, "Interferometric Bell-state preparation using femtosecond-pulse-pumped spontaneous parametric down-conversion," *Phys. Rev. A* **63**, 062301 (2001).
15. Y.-H. Kim and W. P. Grice, "Measurement of the spectral properties of the two-photon state generated via type II spontaneous parametric downconversion," *Opt. Lett.* **30**, 908-910 (2005).
16. A. V. Burlakov, M. V. Chekhova, O. A. Karabutova, and S. P. Kulik, "Biphoton interference with a multimode pump," *Phys. Rev. A* **63**, 053801 (2001).
17. The Wiener-Khinchine theorem states that the spectral power density of an optical field is related to its autocorrelation. They are, in fact, a Fourier transform pair. It is not difficult to show that the following relation holds,  $\Delta\lambda_{\text{FWHM}} = (4\ln 2/\pi)\lambda_{\text{center}}^2/L_{\text{FWHM}}$ . Here  $\Delta\lambda_{\text{FWHM}}$  is the FWHM bandwidth of the field,  $\lambda_{\text{center}}$  is the central wavelength of the laser (405 nm), and  $L_{\text{FWHM}}$  is the FWHM width of the autocorrelation (interferogram) in Fig. 2.
18. J. W. Goodman, *Statistical optics*, (Wiley, New York, 1985), p. 230.
19. S.-Y. Baek, O. Kwon, and Y.-H. Kim, "High-Resolution Mode-Spacing Measurement of the Blue-Violet Diode Laser Using Interference of Fields Created with Time Delays Greater than the Coherence Time," *Jpn. J. Appl. Phys.* **46**, 7720-7723 (2007).
20. Y. J. Lu, R. L. Campbell, and Z. Y. Ou, "Mode-locked two-photon states," *Phys. Rev. Lett.* **91**, 163602 (2003).
21. M. A. Sagioro, C. Olindo, C. H. Monken, and S. Pádua, "Time control of two-photon interference," *Phys. Rev. A* **69**, 053817 (2004).
22. A. Zavatta, S. Viciani, and M. Bellini, "Recurrent fourth-order interference dips and peaks with a comblike two-photon entangled state," *Phys. Rev. A* **70**, 023806 (2004).
23. C. K. Hong, Z. Y. Ou, and L. Mandel, "Measurement of subpicosecond time intervals between two photons by interference," *Phys. Rev. Lett.* **59**, 2044-2046 (1987).
24. J. Jacobson, G. Bjork, I. Chuang, and Y. Yamamoto, "Photonic de Broglie waves," *Phys. Rev. Lett.* **74**, 4835-4838 (1995).
25. K. Edamatsu, R. Shimizu, and T. Itoh, "Measurement of the Photonic de Broglie Wavelength of Entangled Photon Pairs Generated by Spontaneous Parametric Down-Conversion," *Phys. Rev. Lett.* **89**, 213601 (2002).
26. J. G. Rarity, P. R. Tapster, E. Jakeman, T. Larchuk, R. A. Campos, M. C. Teich, and B. E. A. Saleh, "Two-photon interference in a Mach-Zehnder interferometer," *Phys. Rev. Lett.* **65**, 1348-1351 (1990).
27. Z. Y. Ou, X. Y. Zou, L. J. Wang, and L. Mandel, "Experiment on nonclassical fourth-order interference," *Phys. Rev. A* **42**, 2957-2965 (1990).
28. J. Brendel, N. Gisin, W. Tittel, and H. Zbinden, "Pulsed Energy-Time Entangled Twin-Photon Source for Quantum Communication," *Phys. Rev. Lett.* **82**, 2594-2597 (1999).
29. Y.-H. Kim, V. Berardi, M. V. Chekhova, A. Garuccio, and Y. H. Shih, "Temporal indistinguishability and quantum interference," *Phys. Rev. A* **62**, 43820 (2000).
30. S.-Y. Baek and Y.-H. Kim, "Spectral properties of entangled photon pairs generated via frequency-degenerate type-I spontaneous parametric down-conversion," *Phys. Rev. A* **77**, 043807 (2008).
31. We have measured the transmission function of the interference filters used in this experiment with an Agilent 8453 UV/VIS spectro-photometer. We have found that the transmission function is indeed very close Gaussian centered at 810 nm as assumed in eq. (10).

## 1. Introduction

Quantum entanglement is at the heart of newly emerging quantum technologies [1]. In particular, entangled states of photons play essential roles in photon-based quantum technologies, such as, photonic quantum information, quantum communication, quantum cryptography, quantum metrology, etc [2, 3].

Among currently available schemes for generating entangled states of two photons experimentally, by far, spontaneous parametric down-conversion (SPDC), in which a higher energy pump photon is spontaneously split into a pair of lower energy photons due to  $\chi^{(2)}$  nonlinear interactions, offers the most versatile and efficient method of generating entangled two-photon states. For example, entanglement in a variety of degrees of freedom (polarization, position-momentum, phase-momentum, energy-time, etc.) has been demonstrated with SPDC photons [4, 5, 6, 7, 8]. Furthermore, engineered entangled photon sources are possible by taking ad-

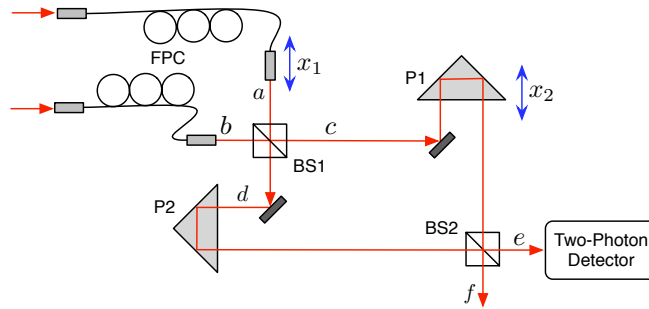


Fig. 1. Schematic of the experiment. FPC is a fiber polarization controller and P1/P2 are trombone prisms. BS1/BS2 are 50:50 beam splitters. Note that  $x_1$  and  $x_2$  should be understood as path length differences.

vantage of the fact that the spectral and temporal properties of SPDC photons depend heavily on the phase matching conditions, the choice of the  $\chi^{(2)}$  medium, and the pumping conditions [9, 10, 11, 12].

As for the phase matching condition, the SPDC process can be characterized with the polarization (type-I and type-II), frequency (degenerate and nondegenerate), and propagation (collinear and noncollinear) properties of the photon pair. The  $\chi^{(2)}$  medium choices include bulk nonlinear crystals, wave-guide type crystals, periodically-poled crystals, and a nonlinear crystal in a cavity. Finally, the SPDC process may be pumped with a continuous wave (cw) laser or a (ultrafast) pulsed laser.

With regard to the pumping conditions, in particular, there exist numerous studies on the properties of SPDC photons generated with the monochromatic pump laser and with the ultrafast broadband (mode-locked) pump laser [4, 5, 6, 13, 14, 15]. The studies on interference properties of SPDC photons generated with the multi-mode cw pump laser, however, are lacking. To the best of our knowledge, Ref. [16] is the only paper, to date, that reports an interferometric effect due to multi-mode cw pumped SPDC: a biphoton interference revival effect, similar to mode-locked ultrafast pumped SPDC, has been observed with a Michelson interferometer using the multi-mode cw pumped SPDC.

This lack of study on multi-mode cw pumped SPDC is largely due to the fact that, in the past, only mainframe ion lasers could offer enough pumping power at the desired pumping wavelength (350 ~ 400 nm). Due to the long cavity length and relatively narrow bandwidth of the mainframe ion lasers, it is actually difficult to observe a uniquely multi-mode effect in the biphoton interference [16]. With the rapid development of inexpensive high-power blue diode lasers (easily providing over 100 mW at 405 nm) in the recent years, however, the multi-mode cw laser pumped SPDC is expected to become an important entangled photon source in photonic quantum information experiments and more and more widely used.

In this paper, we report experimental and theoretical studies on the coherence properties of SPDC photon pairs generated with a multimode cw laser as the pump. By using a Mach-Zehnder interferometer with the SPDC photon pairs at the input ports, both the Hong-Ou-Mandel interference and the photonic de Broglie wave interference have been studied. Our study shows that the multi-mode property of the pump laser is not exhibited in the Hong-Ou-Mandel interference but it appears in the photonic de Broglie wave interference as periodic recurrence of the wave packet. The theoretical analysis, taking into consideration of the multi-mode nature of the pump, is in excellent agreement with the experimental observations.

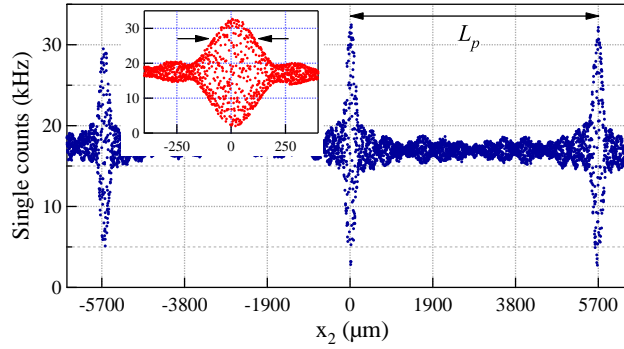


Fig. 2. Coherence property of the pump laser, studied with a Mach-Zehnder interferometer. Periodic recurrence of interference is observed. Inset shows the wave packet around  $x_2 = 0$ .

## 2. Coherence properties of the multimode diode laser

We begin our study by investigating the coherence properties of the pump laser, which is a multimode cw blue laser diode operating at 110 mW. The wavelength of the laser is measured to be 405 nm. To measure the spectral bandwidth of the laser using the Mach-Zehnder interferometer shown in Fig. 1, we send the 405 nm laser via the input mode  $a$  and monitor the output mode  $f$  as a function of  $x_2$ . Note that the input mode  $b$  is not used in this measurement.

The result of the pump coherence measurement using the Mach-Zehnder interferometer is shown in Fig. 2. When the interferometer is scanned around the balanced position,  $x_2 = 0$ , a well-known interference pattern is observed in the single-photon detector placed in the output mode  $f$ . (We attenuated the laser beam with neutral density filters so that we can utilize single-photon detectors.) The envelope of the interference pattern around  $x_2 = 0$  provides the spectral bandwidth of the laser. Given that the full width at half maximum (FWHM) value of the central wave packet is  $216 \mu\text{m}$ , we estimate that the pump laser has the FWHM spectral bandwidth of  $0.67 \text{ nm}$  [17].

The interference recurrence observed in Fig. 2 is due to the multi-mode nature of the cw diode laser and we can make use of this information to evaluate the spacing between the longitudinal modes [18, 19]. Using the peak separation  $L_p = 5668 \mu\text{m}$ , the mode spacing is calculated to be  $\Delta\lambda = \lambda_0^2/L_p = 0.0282 \text{ nm}$  [19]. There are, therefore, roughly 24 longitudinal modes within the FWHM spectrum of the blue diode laser used in this experiment.

The coherence properties of the diode laser can be studied theoretically as follows. Since we have attenuated the intensity of the laser beam severely so that it can be detected with single-photon detectors, we describe the pump photon with the density matrix  $\rho_p$  which is given as

$$\rho_p = \int d\omega_p \mathcal{S}(\omega_p) |\omega_p\rangle\langle\omega_p|, \quad (1)$$

where  $\mathcal{S}(\omega_p)$  is the spectral power density and should be described as a discrete sum of all the frequency modes weighted by the spectral profile. Thus, the spectral power density function is written as

$$\mathcal{S}(\omega_p) = \frac{\sum_{n=-N}^N \mathcal{S}_0(\omega_p) \delta(\omega_p - \omega_{p0} - n\Delta\omega_p)}{\sum_{n=-N}^N \mathcal{S}_0(\omega_{p0} + n\Delta\omega_p)}, \quad (2)$$

where  $\omega_{p0}$  is the central frequency of the pump,  $\Delta\omega_p$  is the mode spacing, and  $n$  is the mode number. We assume that the spectral profile is Gaussian,

$$\mathcal{S}_0(\omega_p) \equiv \exp\left(-(\omega_p - \omega_{p0})^2/2\delta\omega_p^2\right), \quad (3)$$

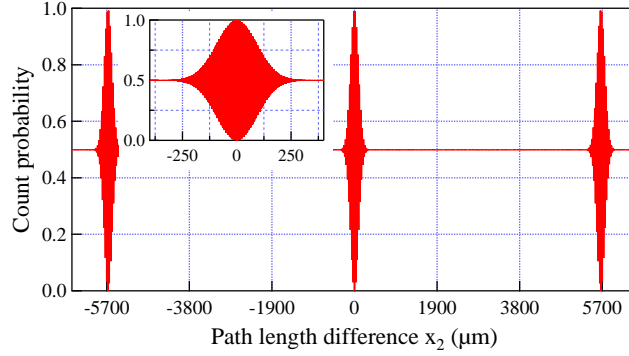


Fig. 3. Coherence property of the pump laser, calculated with eq. (5).  $N = 30$  was used for evaluating the detection probability. Inset shows the wave packet around  $x_2 = 0$ .

where  $\delta\omega_p$  is the pump bandwidth.

If the pump photon with the state eq. (1) enters the interferometer via mode  $a$ ,  $|\omega_p\rangle = a^\dagger(\omega_p)|0\rangle$  where  $a^\dagger(\omega_p)$  is the creation operator for a photon of frequency  $\omega_p$  in mode  $a$ . The normalized detection probability for the single-photon detector placed at the output mode  $f$  is given as

$$R_f = \text{tr}[\rho_p E_f^{(-)}(t) E_f^{(+)}(t)], \quad (4)$$

where  $E_f^{(+)}(t) = (iE_a^{(+)}(t - \tau_2) + iE_a^{(+)}(t) + E_b^{(+)}(t - \tau_2) - E_b^{(+)}(t))/2$  with  $\tau_2 = x_2/c$ ,  $E_a^{(+)}(t) = \int d\omega a(\omega) e^{-i\omega t}$ , and  $E_b^{(+)}(t) = \int d\omega b(\omega) e^{-i\omega t}$ . Here  $a(\omega)$  and  $b(\omega)$  are the annihilation operators for a photon of frequency  $\omega$  in modes  $a$  and  $b$ , respectively.

Evaluating the above equation leads to the single-photon detection probability,

$$R_f = \frac{1}{2} + \frac{1}{2} \mathcal{C}_p(\tau_2), \quad (5)$$

where  $\mathcal{C}_p(\tau_2)$  is the coherence function of the multi-mode cw pump laser,

$$\mathcal{C}_p(\tau_2) = \frac{\sum_n \mathcal{S}_0(\omega_{p0} + n\Delta\omega_p) \cos((\omega_{p0} + n\Delta\omega_p)\tau_2)}{\sum_n \mathcal{S}_0(\omega_{p0} + n\Delta\omega_p)}. \quad (6)$$

Since the coherence properties of the single pump photon is identically reflected in the coherence properties of the laser beam, eq. (5) represents interferogram observed at the output of the interferometer. The experimental data in Fig. 2 is in good agreement with the theoretical plot due to eq. (5) shown in Fig. 3.

### 3. Hong-Ou-Mandel interference with multimode-pumped SPDC

The coherence properties of entangled photon pairs generated via spontaneous parametric down-conversion (SPDC) pumped by a multi-mode cw laser are studied experimentally as follows. The pump laser is a blue diode laser discussed in section 2 and it pumps a 3 mm thick type-I BBO crystal, generating a pair of 810 nm centered SPDC photons which propagate at  $\pm 3^\circ$  with respect to the pump. After passing through a narrowband Gaussian interference filter (5 nm FWHM bandwidth), each photon is then coupled into a single-mode optical fiber to clean up the spatial mode. The interference filter had roughly 52% peak transmission at the center wavelength of 810 nm and the single-mode fiber coupling efficiency measured with a

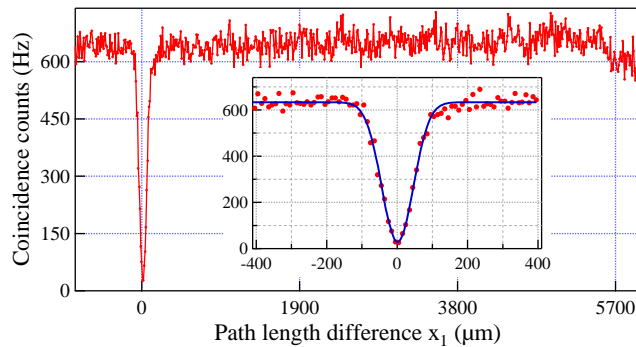


Fig. 4. The coincidence rate  $R_{cd}$  between single-photon detectors in modes  $c$  and  $d$  shows the Hong-Ou-Mandel dip with visibility better than 98%. No recurrence is observed. The single counting rates are roughly 43 kHz and 41 kHz for the single-photon detectors in mode  $c$  and in mode  $d$ , respectively.

He-Ne laser was 61%. The collimated outputs of the single-mode fibers are placed at the input ports of the Mach-Zehnder interferometer as shown in Fig. 1. The relative arrival time of the pair photons at the input beam splitter (BS1) of the Mach-Zehnder interferometer is controlled by moving the output collimator in mode  $a$  in the axial direction ( $x_1$ ). The fiber polarization controllers (FPC) are used to ensure that the polarization states of the photons are identical at the input ports of the interferometer.

Given that the pump laser has recurring periodic temporal coherence, we first investigate the biphoton interference effect at a beam splitter, known as the Hong-Ou-Mandel interference, to see whether the periodic recurring temporal coherence of the pump laser is passed on the Hong-Ou-Mandel type biphoton interference. Note that recurring biphoton Hong-Ou-Mandel type interference has been observed with monochromatic cw laser pumped SPDC filtered with a Fabry-Perot cavity [20, 21, 22].

For this measurement, a single-photon detector (Perkin-Elmer SPCM-AQ4C) is placed in each output mode of BS1 ( $c$  and  $d$ ), and the coincidence counting rate between the two detectors is recorded as a function of the relative input delay  $x_1$ . The experimental data are shown in Fig. 4 and it is clear the Hong-Ou-Mandel dip is observed only when the photons arrive the beam splitter BS1 simultaneously [23]. Unlike Ref. [20, 21, 22] no periodically recurring Hong-Ou-Mandel dip is observed.

#### 4. Photonic de Broglie wave interference with multimode-pumped SPDC

We now study the biphoton photonic de Broglie wave interference by using a Mach-Zehnder interferometer [24, 25]. The SPDC pair photons are sent to the different input ports,  $a$  and  $b$ , of the interferometer and the relative input time delay  $t_1 = x_1/c$  is adjusted by axially moving one output collimator of the single-mode fiber. A two-photon detector, consisting of a 50:50 beam splitter, two single-photon detectors, and a coincidence circuit with a 3 ns coincidence window, is placed at the output mode  $e$  of the interferometer, as shown in Fig. 1. The output of the two-photon detector (i.e., the coincidence count rate) is recorded as functions of  $x_1$  and  $x_2$ . Note that, for observing the photonic de Broglie wave interference, it is necessary to put a two-photon detector at one output port of the interferometer [25]. The coincidence between the single-photon detector located at each output port of the interferometer does not reflect the photonic de Broglie wave interference [25, 26, 27].

The experimental data for the biphoton photonic de Broglie wave interference measurements

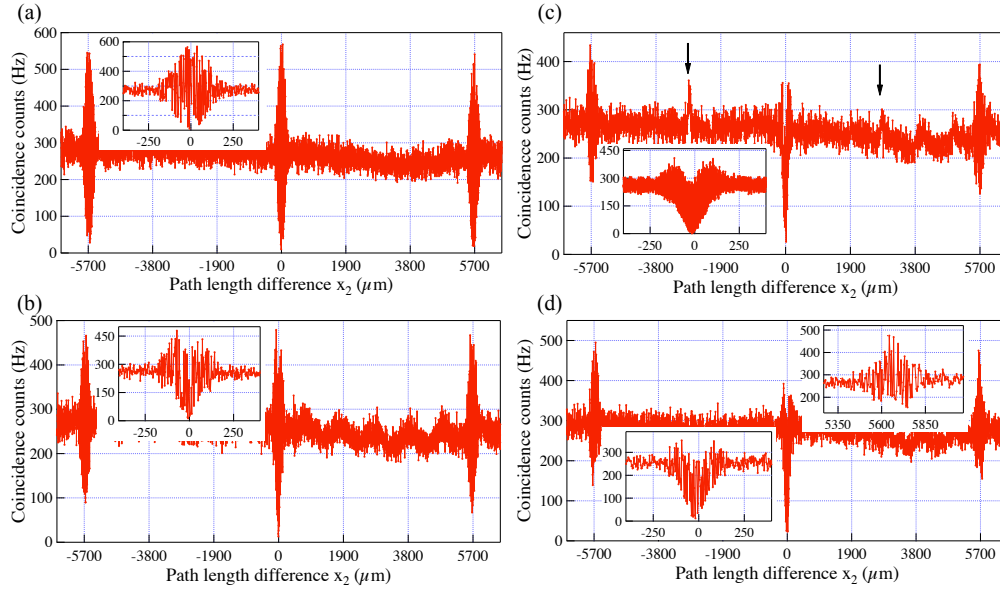


Fig. 5. The biphoton de Broglie wave packet measurement with different  $x_1$  values. (a)  $x_1 = 0 \mu\text{m}$ , (b)  $x_1 = 73 \mu\text{m}$ , (c)  $x_1 = 2834 \mu\text{m}$ , and (d)  $x_1 = 5668 \mu\text{m}$ . While the wave packet shapes are different, the modulation periods are the same in all cases at 405 nm. Note that the visibilities of the central wave packets are roughly the same at 98%.

are shown in Fig. 5. In Fig. 5(a), the biphoton interference is measured as a function of  $x_2$  with the condition  $x_1 = 0 \mu\text{m}$ . Note that, at this condition, the scheme is equivalent to measuring the biphoton photonic de Broglie wavelength as  $x_1 = 0 \mu\text{m}$  condition leads to the photon number-path entangled state or the NOON state,

$$|\psi\rangle_{cd} = (|2\rangle_c|0\rangle_d + |0\rangle_c|2\rangle_d)/\sqrt{2}, \quad (7)$$

in the Mach-Zehnder interferometer as evidenced in Fig. 4.

The biphoton interference reported in Fig. 5(a) exhibits a number of interesting features. First, biphoton wave packets are observed to be periodically recurring at  $x_2 = L_p$ , where  $L_p$  is shown in Fig. 2. Second, the shapes of the individual wave packets are nearly identical to the pump wave packet demonstrated in Fig. 2. Third, the interference fringes exhibit the maximum visibility of  $\sim 98\%$  and the period of oscillation is  $\lambda/N$  ( $N = 2$ ), which is a signature of the biphoton NOON state. The data, therefore, suggest that the pump coherence properties are completely transferred to the biphoton de Broglie wave interference. Note that the biphoton interference revival phenomena reported in Fig. 5(a) is somewhat analogous to the biphoton interference with SPDC generated from mode-locked ultrafast pump pulses where  $L_p/c$  is the time interval between adjacent pulses [16, 28, 29]. The periodic revival of biphoton coherence of multimode-pumped SPDC should have a number of interesting applications in quantum optics, including quantum cryptography, developing an inexpensive ultrabright source of entangled photons, etc, as it offers a way to add biphoton amplitudes coherently or incoherently.

Let us now examine the biphoton de Broglie wave interference when the relative input delay is non-zero,  $x_1 \neq 0$ . These data are reported in Fig. 5(b), Fig. 5(c), and Fig. 5(d) and they correspond to the conditions  $x_1 = 73 \mu\text{m}$ ,  $x_1 = 2834 \mu\text{m}$ , and  $x_1 = 5668 \mu\text{m}$ , respectively. For  $x_1 = 50 \mu\text{m}$ , the pair photons do not arrive at the interferometer simultaneously, but still within

the coherence time (see Fig. 4). The conditions  $x_1 = 2834 \mu\text{m}$  and  $x_1 = 5668 \mu\text{m}$  roughly correspond to  $x_1 \approx L_p/2$  and  $x_1 \approx L_p$ , respectively.

We note a couple of interesting features in the data sets. First, the periodic recurrence of biphoton interference is still observed, regardless of the input delay. Second, the shapes of the central wave packets (near  $x_2 = 0$ ) become asymmetrical (with respect to the random coincidence rate). The side peaks (recurring biphoton wave packets) also become asymmetrical but in the opposite sense, see Fig. 5(d). Third, the visibilities of the central wave packets, interestingly, remain the same as that of Fig. 5(a). The side-peaks, however, start to lose visibilities. It is also interesting to note that two small peaks (without modulations) appear where  $x_2 = \pm x_1$ , marked with arrows in Fig. 5(c).

## 5. Biphoton interference of multimode-pumped SPDC: Theory

In this section, we present a complete theoretical treatment of the experimentally observed biphoton interference with multimode cw-pumped SPDC, reported in Fig. 4 and Fig. 5. We begin by writing the monochromatic laser pumped SPDC two-photon state as [30]

$$|\psi\rangle = \int d\omega_s d\omega_i \delta(\Delta\omega) \text{sinc}(\Delta_k L/2) e^{i\Delta_k L/2} |\omega_s, \omega_i\rangle, \quad (8)$$

where the subscript  $p$  refers to the pump photon. The signal and the idler photons of SPDC are referred with subscripts  $s$  and  $i$ , respectively. Additionally,  $L$  is the thickness of the SPDC crystal,  $\Delta\omega = \omega_p - \omega_s - \omega_i$ , and  $\Delta_k = k_p - k_s - k_i$ .

The pump is a broadband cw laser, consisting of multiple incoherent longitudinal modes. Thus, the SPDC quantum state pumped by the multimode cw laser should be written as,

$$\rho = \int d\omega_p \mathcal{S}(\omega_p) |\psi\rangle\langle\psi|, \quad (9)$$

where the spectral power density of the pump laser  $\mathcal{S}(\omega_p)$  is defined in eq. (2).

We now write the positive frequency component of the electric field operator in mode  $a$  as  $E_a^{(+)}(t) = \int d\omega a(\omega) \phi(\omega) e^{-i\omega t}$ , where  $a(\omega)$  is the annihilation operator for the signal photon in mode  $a$  and  $E_b^{(+)}(t)$  for the idler photon in mode  $b$  is similarly defined. The filter transmission is assumed

$$\phi(\omega) = \exp(-(\omega - \omega_0)^2 / 2\Delta\omega^2) / \sqrt{\Delta\omega\sqrt{\pi}}, \quad (10)$$

where  $\omega_0$  is the central frequency of the SPDC photon ( $\lambda_0 = 810 \text{ nm}$ ) and  $\int |\phi(\omega)|^2 d\omega = 1$  [31].

Let us first consider the Hong-Ou-Mandel interference observed in Fig. 4. The normalized coincidence count rate  $R_{cd}$  between the single-photon detectors in modes  $c$  and  $d$  is proportional to,

$$R_{cd} \propto \int d\tau \text{tr}[\rho E_c^{(-)}(t) E_d^{(-)}(t + \tau) E_d^{(+)}(t + \tau) E_c^{(+)}(t)], \quad (11)$$

where  $E_c^{(+)}(t) = (iE_a^{(+)}(t - \tau_1) + E_b^{(+)}(t)) / \sqrt{2}$ ,  $E_d^{(+)}(t) = (E_a^{(+)}(t - \tau_1) + iE_b^{(+)}(t)) / \sqrt{2}$ , and  $\tau_1 = x_1/c$ . Since, in our experiment, the natural bandwidth of SPDC,  $\text{sinc}(\Delta_k L/2)$ , is much broader than the spectral filter bandwidth  $\Delta\omega$ , the above equation is calculated to be

$$R_{cd} = 1 - \exp(-\Delta\omega^2 \tau_1^2 / 2). \quad (12)$$

This result shows that the Hong-Ou-Mandel interference, when narrowband spectral filtering is done, does not depend on the pump spectrum  $\mathcal{S}(\omega_p)$ . Since the pump coherence function  $\mathcal{C}_p$

does not appear in eq. (12), the Hong-Ou-Mandel interference does not show periodic recurrence. In fact, in this case, the Hong-Ou-Mandel interference is only related to the bandwidth of the spectral filter  $\Delta\omega$ , just as in the case of monochromatic-pumped SPDC with narrowband filtering. It is interesting to note that periodic recurrence of Hong-Ou-Mandel interference can occur by filtering the monochromatic-pumped SPDC with a Fabry-Perot cavity [20, 21, 22].

Let us now describe the photonic de Broglie wave interference measurements with the two-photon detector, as in Fig. 1. The normalized output of the two-photon detector in the output mode  $e$  of the Mach-Zehnder interferometer  $R_{ee}$  is proportional to

$$R_{ee} \propto \int d\tau \operatorname{tr} \left[ \rho E_e^{(-)}(t) E_e^{(-)}(t + \tau) E_e^{(+)}(t + \tau) E_e^{(+)}(t) \right], \quad (13)$$

where  $E_e^{(+)}(t) = (iE_c^{(+)}(t) + E_d^{(+)}(t - \tau_2))/\sqrt{2}$ .

If we were to consider the single-mode pump with frequency  $\omega_p$ , the above expression is reduced to

$$\mathcal{R}_{ee}^s(\omega_p) \propto \int d\tau |\langle 0 | E_e^{(+)}(t + \tau) E_e^{(+)}(t) | \Psi \rangle|^2, \quad (14)$$

and is calculated to be

$$\begin{aligned} \mathcal{R}_{ee}^s(\omega_p) &= 1 + \frac{1}{4} \exp(-(\tau_1 - \tau_2)^2 \Delta\omega^2 / 2) \\ &+ \frac{1}{4} \exp(-(\tau_1 + \tau_2)^2 \Delta\omega^2 / 2) - \frac{1}{2} \exp(-\tau_2^2 \Delta\omega^2 / 2) \\ &- \frac{1}{2} \cos(\omega_p \tau_2) \times (1 + \exp(-\tau_1^2 \Delta\omega^2 / 2)). \end{aligned} \quad (15)$$

Equation (15) shows that when  $\tau_1 = 0$  (i.e., the NOON state interferometer),

$$\mathcal{R}_{ee}^s(\tau_1 = 0) = 1 - \cos(\omega_p \tau_2). \quad (16)$$

Thus, for the monochromatic-pumped SPDC, the biphoton state also behaves monochromatic: the coherence length of the photonic de Broglie wave packet is essentially infinite. For SPDC photon pairs pumped by a narrowband laser, the coherence length of the photonic de Broglie wave packet is equal to that of the pump laser, much bigger than the coherence lengths of the signal and the idler photons individually [25].

Finally, for the multimode cw pumped SPDC, the response of the two-photon detector is given as,

$$R_{ee} = \frac{\sum_n \mathcal{S}_0(\omega_p) \exp(-(\omega_p - 2\omega_0)^2 / 2\Delta\omega^2) \mathcal{R}_{ee}^s(\omega_p)}{\sum_n \mathcal{S}_0(\omega_p)}, \quad (17)$$

where  $\omega_p = \omega_{p0} + n\Delta\omega_p$ . Note that  $\omega_{p0}$  is the central frequency of the pump laser,  $\omega_0$  is the central frequency of the SPDC photon such that  $\omega_{p0} = 2\omega_0$  (i.e., assumed to be degenerate),  $n$  is the mode number,  $\Delta\omega_p$  is the mode spacing, and  $\Delta\omega$  is the bandwidth of the Gaussian spectral filter for the SPDC photons (assumed to be narrower than the natural bandwidth of SPDC).

The normalized output of the two-photon detector is then evaluated to be

$$\begin{aligned} R_{ee} &= 1 + \frac{1}{4} \exp(-(\tau_1 - \tau_2)^2 \Delta\omega^2 / 2) \\ &+ \frac{1}{4} \exp(-(\tau_1 + \tau_2)^2 \Delta\omega^2 / 2) - \frac{1}{2} \exp(-\tau_2^2 \Delta\omega^2 / 2) \\ &- \frac{1}{2} \mathcal{C}_{\text{eff}}(\tau_2) (1 + \exp(-\tau_1^2 \Delta\omega^2 / 2)), \end{aligned} \quad (18)$$

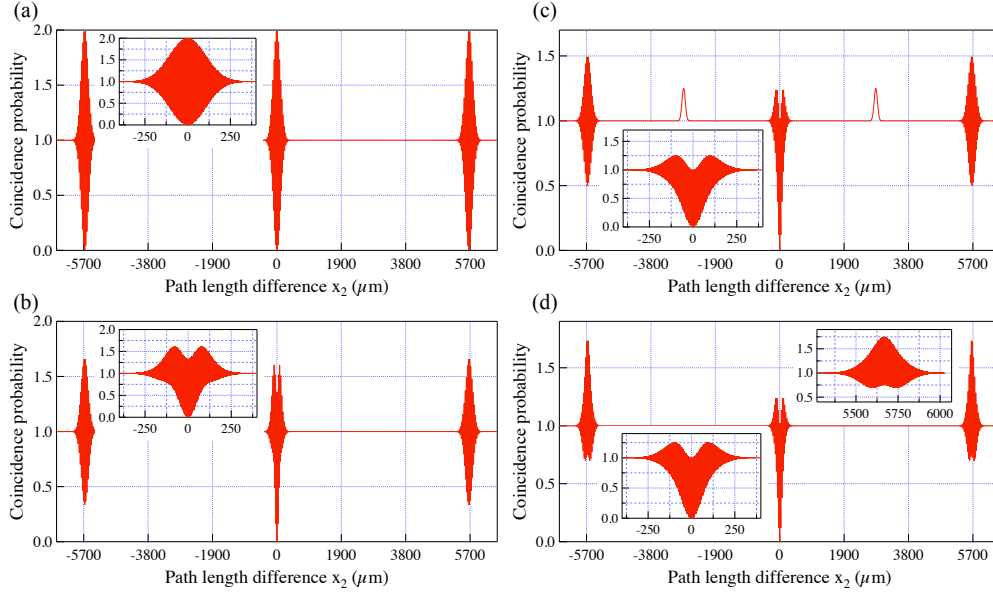


Fig. 6. Theoretical photonic de Broglie wave interference plotted using eq. (18) with  $N = 30$ . The conditions are (a)  $x_1 = 0 \mu\text{m}$ , (b)  $x_1 = 73 \mu\text{m}$ , (c)  $x_1 = 2834 \mu\text{m}$ , and (d)  $x_1 = 5668 \mu\text{m}$ . The theoretical plots are in excellent agreement with the experimental data in Fig. 5.

where the effective coherence function  $\mathcal{C}_{\text{eff}}(\tau_2)$  is defined similarly to eq. (6),

$$\mathcal{C}_{\text{eff}}(\tau_2) = \frac{\sum_n \mathcal{S}_{\text{eff}}(\omega_{p0} + n\Delta\omega_p) \cos((\omega_{p0} + n\Delta\omega_p)\tau_2)}{\sum_n \mathcal{S}_{\text{eff}}(\omega_{p0} + n\Delta\omega_p)}, \quad (19)$$

where  $\mathcal{S}_{\text{eff}}(\omega_p) = \exp(-(\omega_p - 2\omega_0)^2 / \Delta\omega_e^2)$  with  $1/\Delta\omega_e^2 = 1/2\delta\omega_p^2 + 1/2\Delta\omega^2$ . Note again that  $2\omega_0 = \omega_{p0}$  and  $\delta\omega_p$  is the bandwidth of the pump laser.

Equation (18) predicts that the output of the two-photon detector would exhibit the biphoton photonic de Broglie wave interference,  $\lambda/N$  ( $N = 2$ ) modulation, and the shape of the wave packet is determined by  $\tau_1$ ,  $\tau_2$ , and  $\Delta\omega$ . Equation (18) is plotted in Fig. 6 for comparison with the experimental data in Fig. 5. The theoretical description of the biphoton interference of multimode cw-pumped SPDC is thus in excellent agreement with the experimental observation.

## 6. Conclusion

We have studied quantum interference effects of multimode cw-laser pumped spontaneous parametric down-conversion by using a Mach-Zehnder interferometer and a two-photon detector. Both the Hong-Ou-Mandel interference and the photonic de Broglie wave interference are studied. The multi-mode property of the pump laser does not show up in the Hong-Ou-Mandel interference, but it is reflected on the biphoton photonic de Broglie wave interference as periodic recurrence of the wave packet, closely resembling the coherence properties of the multi-mode pump. In addition, the recurring wave packet shapes are shown to be dependent on the arrival time delay between the photon pair at the input beam splitter of the Mach-Zehnder interferometer. The theoretical analysis, taking into consideration of the multi-mode nature of the pump, is in excellent agreement with the experimental observations.

The present study offers an insight on how to add biphoton amplitudes coherently/incoherently for the two-photon states generated with a multimode cw pump laser, such

as a compact blue diode laser. We, therefore, believe that coherence properties of multimode cw pumped SPDC, reported in this paper, should be applicable, for example, in quantum cryptography, engineered entangled photon sources, compact ultrabright entangled photon sources, where inexpensive blue diode lasers are used as the pump source for SPDC.

### **Acknowledgements**

This work was supported by the Korea Research Foundation (KRF-2006-312-C00551), the Korea Science and Engineering Foundation (2009-0070668), and the Ministry of Knowledge and Economy of Korea through the Ultrashort Quantum Beam Facility Program.